J|A|C|S
ARTICLES
Published on Web 04/13/2007

Design of Liquid-Crystalline Aqueous Suspensions of Rutile Nanorods: Evidence of Anisotropic Photocatalytic Properties

Arnaud Dessombz,[†] David Chiche,[‡] Patrick Davidson,*[,†] Pierre Panine,[§] Corinne Chanéac,*[,‡] and Jean-Pierre Jolivet[‡]

Contribution from the Laboratoire de Physique des Solides, UMR CNRS 8502, Bâtiment 510, Université Paris-Sud, 91405 Orsay, France, Laboratoire de Chimie de la Matière Condensée, UMR CNRS 7574, Université Paris 6, 4 Place Jussieu, 75252 Paris, France, and European Synchrotron Radiation Facility, B.P.220, 38043 Grenoble, France

Received November 24, 2006; Revised Manuscript Received March 12, 2007; E-mail: chaneac@ccr.jussieu.fr; davidson@lps.u-psud.fr

Abstract: TiO_2 rutile nanorods of average length $L = 160 \pm 40$ nm and average diameter $D = 15 \pm 5$ nm have been synthesized through a seed-mediated growth process by $TiCl_4$ hydrolysis in concentrated acidic solution. These nanorods were dispersed in water to yield stable (aggregation-free) colloidal aqueous suspensions. At volume fractions $\phi > 3\%$, the suspensions spontaneously display a phase separation into an isotropic liquid phase and a liquid-crystalline phase identified as nematic by X-ray scattering. At $\phi > 12\%$, the suspensions form a nematic single phase, with large order parameter, $S = 0.75 \pm 0.05$. Very well aligned rutile films on glass substrate were produced by spin-coating, and their photocatalytic properties were examined by monitoring the decomposition of methylene blue under UV light. We found that UV-light polarized along the quadratic axis of the rutile nanorods was most efficient for this photocatalytic reaction.

Introduction

The field of mineral liquid crystals (i.e., colloidal liquid-crystalline suspensions of mineral anisotropic nanoparticles) has recently attracted renewed interest because these suspensions may combine the typical fluidity and anisotropic properties of liquid crystals with the usual electronic properties of minerals such as magnetism or electric conductivity.[1] The main types of mesophases, nematic, lamellar, and columnar, composed of mineral particles have already been observed, sometimes even for the same system.[2] Research in this field now focuses on specific materials (boehmite, gibbsite, clays and layered compounds, gold, CdSe, $Ni(OH)_2$, etc.) that are particularly important in an industrial context.[3] The rutile polymorph of TiO_2 is one such material that finds widespread industrial use as pigment, in solar cells, as catalyst support, as photocatalyst, etc.[4] Most of these applications actually involve spherical anatase (another TiO_2 polymorph) or rodlike rutile particles but the formation of liquid-crystalline phases requires very anisotropic particles, free from aggregation. More precisely, the onset of liquid-crystalline order occurs at a concentration that decreases with increasing particle aspect ratio. Besides, achieving good colloidal stability of aqueous suspensions of rutile nanorods is quite challenging. The van der Waals attractions between rutile nanorods are strong[5] because of the large rutile hamaker constant, and the electrostatic repulsions between particles are limited by their electrostatic surface charge density.[6] These difficulties are even more severe in concentrated suspensions where the average distance between nanorods is not very large.

Methods recently developed to obtain anisotropic particles of pure rutile involve hydrothermal[7] or microwave hydrothermal[8] conditions and the use of mineralizers[9] or surfactants.[10] A

[†] Laboratoire de Physique des Solides, UMR CNRS 8502.
[‡] Laboratoire de Chimie de la Matière Condensée, UMR CNRS 7574.
[§] European Synchrotron Radiation Facility.

(1) (a) Gabriel, J. C. P.; Davidson, P. *Adv. Mater.* **2000**, *12*, 9−20. (b) Davidson, P.; Gabriel, J. C. P. *Curr. Opin. Coll. Interf. Sci.* **2005**, *9*, 377−383.
(2) (a) van der Beek, D.; Lekkerkerker, H. N. W. *Langmuir* **2004**, *20*, 8582−8586. (b) Vroege, G. J.; Thies-Weesie, D. M. E.; Petukhov, A. V.; Lemaire, G. J.; Davidson, P. *Adv. Mater.* **2006**, *18*, 2565−2568.
(3) (a) Buining, P. A.; Philipse, A. P.; Lekkerkerker, H. N. W. *Langmuir* **1994**, *10*, 2106−2114. (b) Van der Kooij, F. M.; Kassapidou, K.; Lekkerkerker, H. N. W. *Nature* **2000**, *406*, 868−871. (c) Van der Beek, D.; Petukhov, A. V.; Oversteegen, S. M.; Vroege, G. J.; Lekkerkerker, H. N. W. *Eur. Phys. J. E* **2005**, *16*, 253−258. (d) Miyamoto, N.; Nakato, T. *J. Phys. Chem. B* **2004**, *108*, 6152−6159. (e) Li, L. S.; Walda, J.; Manna, L.; Alivisatos, A. P. *Nano Lett.* **2002**, *2*, 557−560. (f) Li, L. S.; Alivisatos, A. P. *Adv. Mater.* **2003**, *15*, 408−411. (g) Li, L. S.; Marjanska, M.; Park, G. H. J.; Pines, A.; Alivisatos, A. P. *J. Chem. Phys.* **2004**, *120*, 1149−1152. (h) Jana, N. R.; Gearheart, L. A.; Obare, S. O.; Johnson, C. J.; Edler, K. J.; Mann, S.; Murphy, C. J. *J. Mater. Chem.* **2002**, *12*, 2909−2912. (i) Brown, A. B. D.; Clarke, S. M.; Rennie, A. R.; *Langmuir* **1998**, *14*, 3129−3132. (j) Michot, L. J.; Bihannic, I.; Maddi, S.; Funari, S. S.; Baravian, C.; Levitz, P.; Davidson, P. *Proc. Nat. Acad. Sci. U.S.A.* **2006**, *103*, 16101−16104. (k) Liu, S.; Zhang, J.; Wang, N.; Liu, W.; Zhang, C.; Sun, D. *Chem. Mater.* **2003**, *15*, 3240−3241.
(4) (a) Reisch, M. *Chem. Eng. News* **2001**, *79(45)*, 23−30. (b) Sakai, A. *Fragance J.* **2003**, *31* (4), 81−91. (c) Fujishima, A.; Honda, K. *Nature* **1972**, *238*, 37−37. (c) O'Regan, B.; Grätzel, M. *Nature* **1991**, *353*, 737−740. (d) Nakade, N.; Saito, Y.; Kubo, W.; Kitamuara, T.; Wada, Y.; Yanagida, S. *J. Phys. Chem. B* **2003**, *107*, 8607−8611. (e) Garzella, C.; Comini, E.; Tempesti, E.; Frigeri, C.; Sberveglieri, G. *Sens. Actuators, B* **2000**, *68*, 189−196.
(5) Israelachvili, J. N. *Intermolecular and Surface Forces;* Academic: London, 1991.
(6) Jolivet, J. P. *Metal Oxide Chemistry and Synthesis. From Solution to Solid State*, Wiley: Chichester, U.K., 2000.
(7) Zhang, Q.; Gao, L. *Langmuir* **2003**, *19*, 967−971.
(8) Guobin, M. A.; Zhao, X.; Zhu, J. *Int. J. Mod. Phys. B* **2005**, *19*, 2763−2768.
(9) Cheng, H.; Ma, J.; Zhao, Z.; Qi, L. *Chem. Mater.* **1995**, *7*, 663−671.
(10) Tahir, M. N.; Theato, P.; Oberle, P.; Melnyk, G.; Faiss, S.; Kolb, U.; Janshoff, A.; Stepputtat, M.; Tremel, W. *Langmuir* **2006**, *22*, 5209−5212.

 10.1021/ja0684491 CCC: $37.00

simple route for the synthesis of rutile nanorods was recently reported; it involves the hydrolysis of highly concentrated $TiCl_4$ solution in concentrated nitric acid.[11] Using this method, nanorods exhibit a high surface charge density that allows the prevention of aggregation and the production of aqueous dispersions, but the objects are not anisotropic enough to display liquid-crystalline behavior.

Particle shape can also be successfully controlled using the seed-mediated growth process that is commonly used for, for example, gold particles.[12] TiO_2 nanorods have thus been prepared by hydrolysis of $TiCl_4$ in soft acidic conditions in the presence of small amounts of nanometric rutile crystal seeds. This method enhances the crystallization rate but without significant improvement in the aspect ratio compared to the classical method.[13]

Here, we present an original method for the synthesis of long rutile nanorods based on seeding with shorter rodlike particles in very acidic solution. Two steps are involved: The first one uses the synthesis described by Gao et al.[11] and leads to anisotropic nanoparticles. These nanorods, not long enough and hereafter called "seed nanorods", are further used in the second step to produce, by oriented attachment, longer nanoparticles, hereafter called "mesogenic nanorods".

The mesophase was studied by polarized light optical microscopy and small-angle X-ray scattering. It was identified as nematic (i.e., with long-range orientational order but only liquidlike short-range positional order).[14] Its range of thermodynamic stability was determined as a function of concentration. Thanks to the visco-elastic properties, large aligned domains of the nematic phase could be obtained by shear flow and highly oriented coatings of rutile nanorods were also produced. As an application, the photocatalytic properties of these highly anisotropic coatings were examined, using the decomposition of methylene blue under polarized UV light. The highest efficiency was found for UV-light polarization parallel to the quadratic axis of the rutile nanorods.

Results

Nanoparticle Synthesis. The XRD pattern of a mesogenic nanorods powder (Figure 1a) shows that the samples are pure rutile TiO_2. No trace of the anatase or brookite polymorphs is detected. TEM micrographs of seed (Figure 1b) and mesogenic (Figure 1c,d) nanorods show that both kinds of nanoparticles have a rodlike morphology. A significant increase of particle length, along the [001] growth direction, was observed after seeding (Figure 1e). The growth process tends to maximize the lateral (110) faces because these faces are the most stable.[15] Both the seed and mesogenic nanorods are quite polydisperse in size. Measurements made on 120 seed nanorods indicate an average length $L = 100 \pm 20$ nm and average diameter $D = 12 \pm 2$ nm, which corresponds to an aspect ratio $L/D \approx 8$. In contrast, the measurements of 150 mesogenic nanorods lead to $L = 160 \pm 40$ nm and $D = 15 \pm 5$ nm, corresponding to an aspect ratio $L/D \approx 11$.

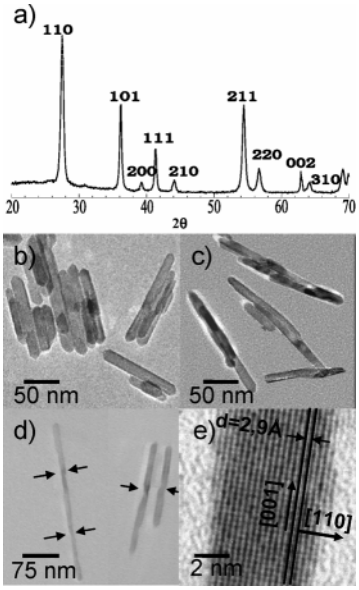

Figure 1. (a) XRD diffractogram of a mesogenic nanorods powder ($\lambda_{Cu}-K_\alpha$). Electron micrographs of rutile nanoparticles precipitated in very acidic conditions showing (b) seed nanorods, (c) aggregated mesogenic nanorods, and (d) well dispersed mesogenic nanorods. The arrows point to the junctions between primary nanoparticles. Panel e shows lattice planes of rutile phase.

Polarized Light Microscopy. Samples of volume fractions ϕ ranging from about 0.03 to 0.12, held in optical flat glass capillaries, spontaneously displayed coexisting isotropic (I) and nematic (N) phases, in good agreement with the first-order character of the I/N transition. A few hours after sample preparation, birefringent droplets (sometimes called "tactoïds") of the nematic phase appear (Figure 2a). Being denser than the isotropic phase, these nematic droplets sediment to the bottom of the capillaries and coalesce into the nematic phase (Figure 2b). After a few days, inspection of the flat capillaries reveals that the phase separation is complete. At volume fractions $\phi <$ 3%, the samples are isotropic, whereas samples at $\phi >$ 12% are entirely nematic. In between, the nematic proportion in the biphasic samples regularly increases with overall volume fraction, as expected (Figure 3). Nematic samples display a very common Schlieren texture (Figure 2c),[14] and the detection of flickering proves that the suspensions are Brownian. Aligned samples were readily obtained by sucking nematic rutile suspensions into flat optical capillaries by using a small vacuum pump. The alignment is illustrated (Figure 2d,e) by comparing the light transmitted when the nematic director is parallel (extinction conditions) to the polarizer axis (or the analyzer) and when the director lies at 45° (maximum transmission) from the polarizer axis.

Small-Angle X-ray Scattering Experiments. Aligned samples of aqueous suspensions of rutile nanorods, held in glass capillaries, are well suited to perform SAXS experiments. Thanks to the large electronic contrast between rutile and water, the scattering signals are very strong (Figure 4a). The SAXS patterns do not display any sharp diffraction lines but anisotropic diffuse scattering is observed instead. Such patterns are actually typical for lyotropic nematic phases comprised of rodlike moieties[16] such as the suspensions of tobacco mosaic viruses. Therefore, the SAXS experiments confirm the nematic nature of the mesophase. A radial scan through the pattern shows that

(11) Huang, Q.; Gao, L. *Chem. Lett.* **2003**, *32*, 638−639.
(12) (a) Brown, K. B.; Walter, D. G.; Natan, M. *J. Chem. Mater.* **2000**, *12*, 306−313. (b) Jana, N. R.; Gearheart, L.; Murphy, C. J. *Adv. Mater.* **2001**, *13*, 1389−1393.
(13) Li, Y.; Fan, Y.; Chen, Y. *J. Mater. Chem.* **2002**, *12*, 1387−1390.
(14) de Gennes, P. G.; Prost, J. *The Physics of Liquid Crystals*, 2nd ed.; Clarendon: Oxford, U.K., 1993.
(15) Li, W. J.; Shi, E. W.; Yin, Z. W. *J. Crystal Growth* **2000**, *208*, 546−554.

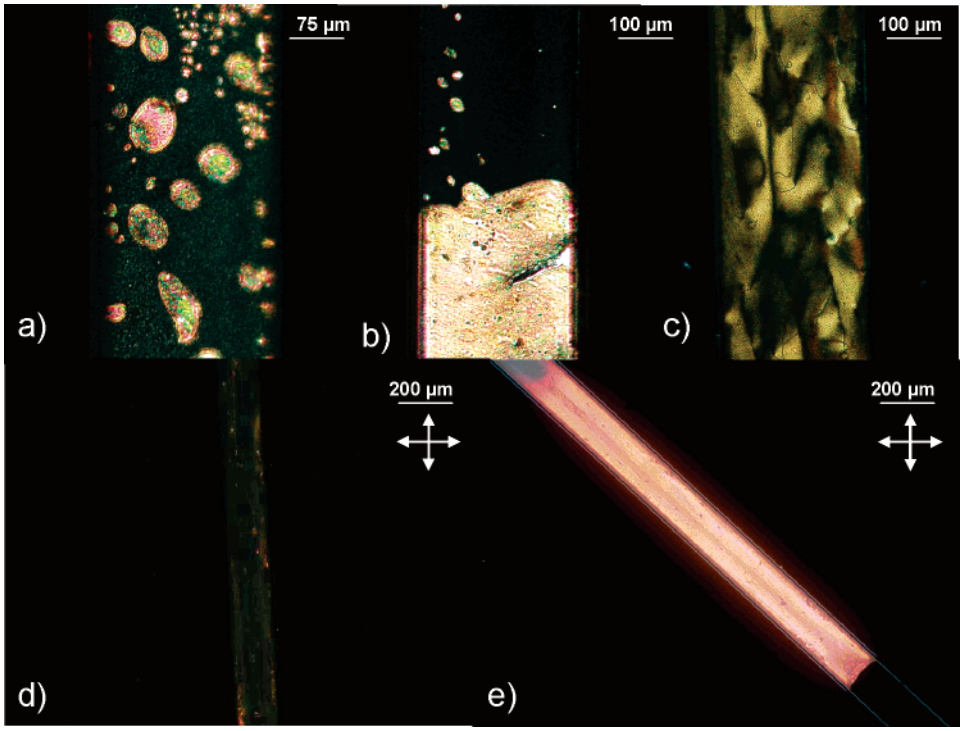

Figure 2. Polarized light microscopy images of concentrated aqueous solutions of rutile mesogenic nanorods held in optical capillaries: (a) nematic droplets forming in the isotropic phase ($\phi = 8.9\%$); (b) biphasic (I/N) sample ($\phi = 8.9\%$); (c) Schlieren texture of the nematic phase ($\phi = 10.6\%$); (d,e) oriented sample ($\phi = 13.3\%$) (d) at 0° and (e) at 45° with respect to the polarizer axis.

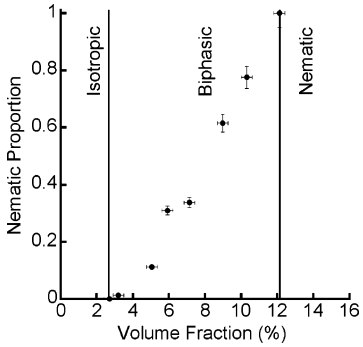

Figure 3. Dependence of the proportion of nematic phase in the suspension with overall volume fraction.

the scattered intensity decreases regularly but exhibits a broad shoulder (Figure 4b). Other SAXS patterns display this scattering more clearly as a broad peak centered on $q = 0.15$ nm^{-1}. It is probably due to the two-dimensional liquidlike positional order of the nanorods and corresponds to a typical distance of $d \approx 40-45$ nm between particles along the planes perpendicular to the director. Such distance agrees reasonably well with the value derived (36 nm) based on the volume fraction, $\phi = 12\%$, and the nanorods diameter, $D = 15$ nm.[17] This shows that the particles are not aggregated but interact through electrostatic repulsions. An azimuthal scan going through the diffuse shoulder (Figure 4c) allowed us, using well-documented methods,[18] to derive the nematic order parameter $S = 0.75 \pm 0.05$ of this aligned sample. This large value agrees well with the first-order character of the I/N transition[19] and shows that the nanorods do not fluctuate much around their common alignment direction in the nematic phase. This experimental result is interesting from a more applied point of view, as illustrated in the next section.

Application to Photocatalysis. Nematic rutile nanorods suspensions were spin-coated onto microscope glass slides and the dried coatings were examined in polarized light microscopy. Coatings obtained from concentrated suspensions ($\phi >$ 7%) are homogeneous and display a uniform radial distribution of the nanorod directions (Figure 5). A small part of coating (dashed triangle in Figure 5) was cut, away from the center, where the director may be considered fairly uniform. This coating of aligned rutile nanorods was then tested for methylene blue decomposition reaction under polarized UV light, using an experimental setup described in Figure 6A. The influence of UV-light polarization was always tested by using the same piece of rutile coating and in the same experimental conditions. A very clear effect of the rutile nanorods orientation with respect to the UV-light polarization was evidenced (Figure 6B). The photocatalytic efficiency of the rutile nanorods is highest when the polarization of the UV light is parallel to the *c*-axis of the nanorods since the degradation of methylene blue is more important in this geometry. This observation was quite reproducible. No variation in efficiency could be detected after 6−8 catalytic tests, over up to 10 h. Proper control experiments were performed in the absence of rutile or of UV light or with a sample made isotropic by rotation (isotropic

(16) (a) Purdie, K. R.; Dogic, Z.; Fraden, S.; Ruhm, A.; Lurio, L.; Mochrie, S. G. *J. Phys. Rev. E* **2003**, *67*, 031708-1−031708-12. (b) Oldenburg, R.; Wen, X.; Meyer, R. B.; Caspar, D. L. D. *Phys. Rev. Lett.* **1988**, *67*, 1851−1854. (c) Keates, P.; Mitchell, G. R.; Peuvrel, E. *Polymer* **1992**, *33*, 3298−3301. (d) Ao, X.; Wen, X.; Meyer, R. B. *Physica A (Amsterdam)* **1991**, *176*, 63−71.
(17) Belamie, E.; Davidson, P.; Giraud-Guille, M. M. *J. Phys. Chem. B* **2004**, *108*, 14991−15000.
(18) (a) Leadbetter, A. J.; Norris, E. K. *Mol. Phys.* **1979**, *38*, 669−686. (b) Davidson, P.; Petermann, D.; Levelut, A. M. *J. Phys. II* **1995**, *5*, 113−131.
(19) (a) Onsager, L. *Ann. N. Y. Acad. Sci.* **1949**, *51*, 627−659. (b) Vroege, G. J.; Lekkerkerker, H. N. W. *Rep. Prog. Phys.* **1992**, *55*, 1241−1309.

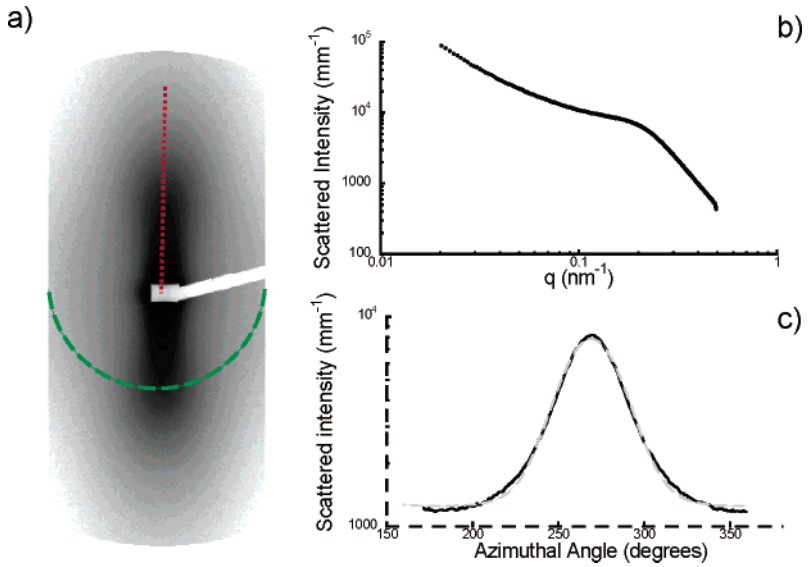

Figure 4. Small-angle X-ray scattering pattern (a) of a flow-aligned nematic sample of rutile suspension ($\phi = 12\%$) and (b) intensity profiles in a radial direction (represented by a dotted straight line on the pattern) and (c) along a (dashed) half-circle. The shoulder on the radial profile is related to the average distance between nanorods, and the azimuthal profile gives the nematic order parameter (see text).

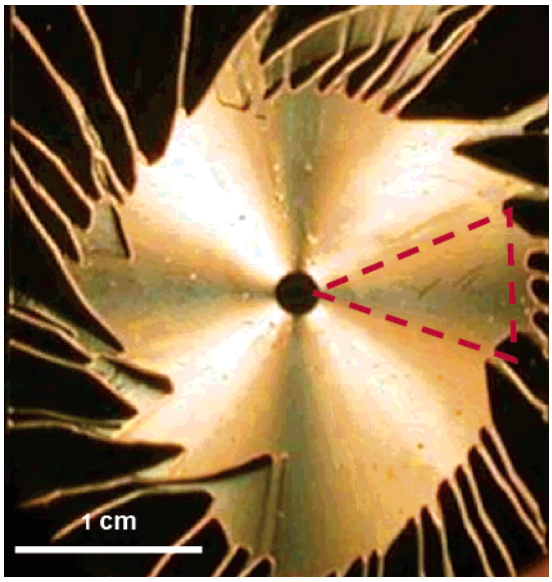

Figure 5. Photograph of the rutile film obtained by spin-coating of a nematic suspension, observed between crossed polarizers. The dashed triangle shows the portion of rutile coating that was cut to perform photocatalysis experiments.

coatings of good quality could not be directly produced). None of these control experiments showed any anisotropy of catalytic efficiency (see Figure S1A, Supporting Information). Applying Beer−Lambert's law[20] allowed us to determine the concentrations, C_{MB}, of methylene blue from the absorption spectra. In our experimental conditions, C_{MB} fell from 10^{-5} M to 3.6×10^{-6} M when the polarization of light was parallel to the *c*-axis, whereas it only fell to 7.6×10^{-6} M when the polarization of light was perpendicular. The kinetics of methylene blue degradation follows a first-order law over a few hours, suggesting that no deactivation can be detected over this time range (see Figure S1B, Supporting Information).

Discussion

In acidic medium, particle growth is promoted compared to nucleation. The nanorod length increases with acidity but this growth is restricted by the occurrence of aggregation in very acidic and concentrated conditions. A solution to increase the length is to resort to seeding which allows control of the nucleation and growth steps, as illustrated here. However, the length increase that we achieved is not simply due to the particle growth. Indeed, we observed the end-to-end attachment of the nanorods which was probably made possible by the continuous introduction of precursors. In this way, we obtained mesogenic nanorods (Figure 1d) that resulted from the oriented attachment of two or three seed nanorods. Similar oriented aggregation phenomena that involve the formation of secondary particles by self-assembly of primary particles were largely described in the literature.[21] This growth process of course increases the polydispersity. A second and beneficial effect of the high acidity is that the electrostatic surface charge density of the nanorods (primary and mesogenic) is large enough to obtain a stable particle dispersion thanks to electrostatic repulsions.

The Onsager model and its subsequent refinements provide a general frame to understand the I/N phase transition.[19] This model, valid for very anisotropic particles that only interact through hard-core repulsions, predicts a strongly first-order phase transition with volume fractions of the isotropic and nematic phases at coexistence given by $\phi_i = 3.3$ D/L and $\phi_n = 4.2$ D/L, respectively. A large jump of nematic order parameter, $S = 0.80$, at the transition is also predicted. Our experimental observations of the phase coexistence and the value of $S = 0.75$ at the transition do agree with these predictions. However, the very wide biphasic gap that ranges from 3% to 12% hints at a very large polydispersity distribution, with the longer nanorods segregating into the most dilute drops of the nematic phase.[22] Applying the above-mentioned formulas for the volume fractions

(20) Bauman, R. P. *Absorption Spectroscopy*; John Wiley & Sons: New York, 1966, pp 368−370.

(21) (a) Penn, R. L. *J. Phys. Chem. B* **2004**, *108*, 12707−12712. (b) Adachi, M.; Murata, Y.; Takao, J.; Jiu, J.; Sakamoto, M.; Wang, F. *J. Am. Chem. Soc.* **2004**, *45*, 14943−14949.

(22) Donkai, N.; Kajiwara, K.; Schmidt, M.; Miyamoto, K. *Makromol. Chem., Rapid Commun.* **1993**, *14*, 611−617.

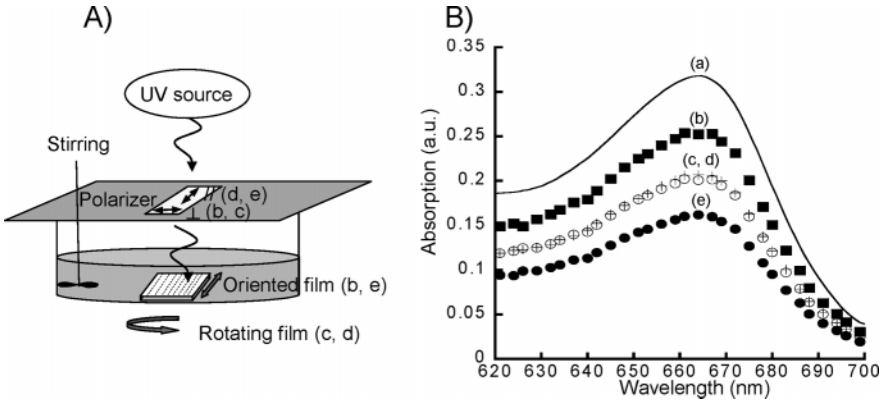

Figure 6. (A) Sketch of the experimental setup used for the photocatalysis experiments. (B) Absorption curves of methylene blue aqueous solutions: (a, solid line) reference with no rutile and no UV irradiation, (b, closed squares) anisotropic rutile coating exposed to UV-light polarized in the direction perpendicular to the nanorods *c*-axis, (c, crosses) isotropic (rotating) rutile coating exposed to UV-light polarized in the same direction as trace b, (d, open circles) isotropic (rotating) rutile coating exposed to UV-light polarized in the direction perpendicular to trace b, (e, closed circles) anisotropic rutile coating exposed to UV-light polarized in the direction parallel to the nanorods *c*-axis.

at coexistence leads to theoretical values ($\phi_i = 28\%$ and $\phi_n = 35\%$) much larger than the center of the biphasic gap found around 8%. However, the Onsager model being only valid in the limit of very anisotropic particles (L/D > 100), a more meaningful comparison should rather be drawn with the numerical simulations of less anisotropic particles, with predicted values around 20%.[23] Moreover, rutile nanorods are actually charged, with mean surface charge densities of 0.2 $C \cdot m^{-2}$, and the effect of electrostatic repulsions, although very difficult to compute precisely,[19] is to decrease appreciably the volume fractions at the transition, here by approximately a factor of 2.

The previous theoretical considerations show that the I/N transition must take place at smaller volume fractions for the mesogenic nanorods of aspect ratio ~11 than for the seed nanorods of aspect ratio ~8. One could however still expect the suspensions of seed nanorods to also form a nematic phase but at a higher volume fraction (by approximately 30%). Actually, when sheared, these suspensions do display streaming birefringence because of the transient alignment of the seed nanorods in the flow. This phenomenon is regarded as a pretransitional effect associated with the possible existence of a nematic phase at higher volume fraction, and the transient alignment may persist for hours. Unfortunately, at the higher volume fractions that must be reached for an aspect ratio of ~8, the seed nanorods aggregate on a time scale of a few days, which prevents the suspension from organizing in a stable nematic phase. Because of the different synthesis conditions, the mesogenic nanorods may also bear a larger electrical charge than the seed nanorods.

Although sol/gel transitions are commonly observed with aqueous suspensions of very anisotropic and charged nanoparticles, no gelation was detected in our experiments. Even at volume fractions as large as 16%, the suspensions are quite viscous but do not make a gel. Therefore, the nematic phase obtained at large volume fractions (ϕ > 12%) is fluid and thermodynamically stable.

Interestingly, coatings obtained from suspensions in the isotropic phase were heterogeneous and of poor quality; they showed no orientation in polarized-light microscopy. In contrast, coatings prepared from biphasic or nematic suspensions were both homogeneous and showed significant nanorods orientation. These experiments therefore illustrate the positive role played by the cooperative nematic ordering in the production of oriented coatings by shear flow. The coating speed, in the range investigated here (2000−6000 rpm), did not influence the quality of the coatings so that the suspension volume fraction appears as the main control parameter.

Our experiments clearly show that rutile photocatalysis is most efficient when the polarization of UV-light is parallel to the *c*-axis of the structure. The understanding and calculation of the electronic band structure of TiO_2 rutile is still an active subject of research.[24] Rutile is regarded as a wide-band-gap semiconductor and a mostly ionic material. Unfortunately, the theoretical methods do not seem accurate enough yet to precisely predict the magnitude and nature (direct or indirect) of the band gap. Moreover, the nature of the nanorods crystalline faces exposed to the solution should also be considered.[25] Besides, the fact that we deal here with nanorods rather than bulk rutile further complicates this issue. Altogether, explaining our results about the light-polarization dependence of the photocatalytic activity therefore seems an interesting theoretical problem.

Conclusion

In this work, using a seed-mediated growth process we have engineered pure rutile nanorods that are elongated enough to organize into a nematic phase when dispersed in water at large volume fractions (ϕ > 12%). This nematic phase is thermodynamically stable, it shows usual nematic textures in polarized-light microscopy and displays typically nematic SAXS patterns. We have presented one example where this liquid-crystalline behavior sheds new light on one of the applications of rutile, that is, its photocatalytic activity. Moreover, the very large refraction index of rutile makes it a very interesting material in liquid-crystal science. In this respect, one may even envision the doping of common thermotropic liquid crystals (used in

(23) Bolhuis, P.; Frenkel, D. *J. Chem. Phys.* **1997**, *106*, 666−687.

(24) (a) Glassford, K. M.; Chelikowsky, J. R. *Phys. Rev. B* **1992**, *46*, 1284−1298. (b) Zhang, Y. F.; Lin, W.; Li, Y.; Ding, K. N.; Li, J. Q. *J. Phys. Chem. B* **2005**, *109*, 19270−19277. (c) Kuo, M. Y.; Chen, C. L.; Hua, C. Y.; Yang, H. C.; Shen, P. Y. *J. Phys. Chem. B* **2005**, *109*, 8693−8700.

(25) Albaret, T.; Finocchi, F.; Noguera, C. *Faraday Discuss.* **1999**, *114*, 285−304.

display technology) with these TiO_2 nanorods, as was previously reported with $BaTiO_3$ ferroelectric nanoparticles.[26]

Acknowledgment. Fabienne Warmont (University Pierre et Marie Curie, Paris) and Dominique Jalabert (University of Orleans) are gratefully acknowledged for help with the transmission electron microscopy experiments. We thank Professor Rudolf Zentel for communicating to us a preprint about suspension in organic solvents of polymer-coated rutile nanorods. We are very grateful to J. Ferré and J. P. Jamet for helpful discussions and the loan of a UV-polarizer.

Supporting Information Available: Experimental details. This material is available free of charge via the Internet at http://pubs.acs.org.

JA0684491

(26) Li, F. H.; Buchnev, O.; Il Cheon, C.; Glushchenko, A.; Reshetnyak, V.; Reznikov, Y.; Sluckin, T. J.; West, J. L. *Phys. Rev. Lett.* **2006**, *97*, 147801-1−147801-4.